Z. Phys. C - Particles and Fields 31, 527–535 (1986)

Zeitschrift für Physik C Particles and Fields

Measurement of the Photon Structure Function F_2^γ at Q^2 from 7 to 70 (GeV/c)^2

TASSO Collaboration

M. Althoff[1], W. Braunschweig, R. Gerhards, F.J. Kirschfink, H.U. Martyn, P. Rosskamp, W. Wallraff

I. Physikalisches Institut der RWTH Aachen, D-5100 Aachen, Federal Republic of Germany[18]

B. Bock, J. Eisenmann, H.M. Fischer, H. Hartmann, W. Hillen[2], A. Jocksch, H. Kolanoski, H. Kück[3], V. Mertens, R. Wedemeyer

Physikalisches Institut der Universität Bonn, D-5300 Bonn, Federal Republic of Germany[18]

B. Foster

H.H. Wills Physics Lab., University of Bristol, Bristol BS8 1TL, UK[19]

E. Bernardi, Y. Eisenberg[4], A. Eskreys[5], K. Gather, H. Hultschig, P. Joos, B. Klima, H. Kowalski, A. Ladage, B. Löhr, D. Lueke, P. Mättig[6], D. Notz, D. Revel[4], E. Ronat[4], D. Trines, T. Tymieniecka[7], R. Walczak[8], G. Wolf, W. Zeuner

Deutsches Elektronen-Synchrotron, DESY, D-2000 Hamburg, Federal Republic of Germany

E. Hilger, T. Kracht, H.L. Krasemann[9], J. Krüger, E. Lohrmann, G. Poelz, K.U. Pösnecker

II. Institut für Experimentalphysik der Universität Hamburg, D-2000 Hamburg, Federal Republic of Germany[18]

D.M. Binnie, P.J. Dornan, D.A. Garbutt, C. Jenkins, W.G. Jones, J.K. Sedgbeer, D. Su, J. Thomas[10], W.A.T. Wan Abdullah[11]

Department of Physics, Imperial College, London SW7 2AZ, UK[19]

F. Barreiro, E. Ros

Universidad Autonoma de Madrid, Madrid, Spain[20]

M.G. Bowler, P. Bull[12], R.J. Cashmore, P. Dauncey, R. Devenish, G. Heath, D.J. Mellor

Department of Nuclear Physics, Oxford University, Oxford OX1 3RH, UK[19]

S.L. Lloyd

Department of Physics, Queen Mary College, London E1 4NS, UK[19]

G.E. Forden, J.C. Hart, D.K. Hasell, D.H. Saxon

Rutherford Appleton Laboratory, Chilton, Oxon, OX11 OQX, UK[19]

S. Brandt, M. Dittmar[10], M. Holder, L. Labarga[13], B. Neumann

Fachbereich Physik der Universität-Gesamthochschule Siegen, D-5900 Siegen, Federal Republic of Germany[18]

U. Karshon, G. Mikenberg, A. Montag, R. Mir, A. Shapira, G. Yekutieli

Weizmann Institute, Rehovot 76100, Israel[21]

G. Baranko, A. Caldwell, M. Cherney[14], J.M. Izen[15], S. Ritz, D. Strom, M. Takashima, H. Venkataramania[16], E. Wicklund[17], Sau Lan Wu, G. Zobernig

Department of Physics, University of Wisconsin, Madison, WI 53706, USA[22]

Received 18 March 1986

Abstract. We have measured the process $e^+e^- \to e^+e^-$ + hadrons, where one of the scattered electrons was detected at large angles, with Q^2 ranging from 7 to 70 (GeV/c)^2. The photon structure function $F_2^\gamma(x, Q^2)$ was determined at an average Q^2 of 23 (GeV/c)^2. The measurements were compared to theoretical predictions of the Quark Parton Model and Quantum Chromodynamics. In both models a hadronic part was added. Within the errors the data are in agreement with the QPM using quark masses of 300 MeV/c^2 for the light quarks. The data also agree with a QCD calculation including higher order corrections. A fit yielded a $\Lambda_{\overline{\text{MS}}}$ value of 140^{+190}_{-65} MeV, where the errors include statistical and systematic uncertainties.

1. Introduction

At e^+e^- storage rings the two-photon production of hadrons in the reaction

$$e^+e^- \to e^+e^- + \text{hadrons} \tag{1}$$

provides the possibility to study the structure functions of the photon. Reaction (1) can be interpreted as deep inelastic $e\gamma$ scattering in the case where one of the incoming electrons is scattered at a large angle θ_1 and the other one restricted to small angles θ_2. In this configuration the highly virtual photon with the four-momentum transfer squared $|q^2| \gg 0$ probes the structure of the other quasi real photon (target photon) with a four-momentum transfer squared $|p^2|$ close to zero.

We have measured process (1) with the TASSO detector at beam energies, E_b, between 16.5 GeV and 17.5 GeV. The total integrated luminosity collected was 52.5 pb^{-1}. One of the scattered electrons was detected at large angles (single tag condition). The data were analyzed in terms of the photon structure function F_2^γ. Measurements of F_2^γ have been published earlier by the PLUTO, JADE and CELLO collaborations [1-3].

2. Theoretical Framework

For quasi real target photons the cross section of process (1) can be expressed in terms of the two structure functions $F_1^\gamma(x, Q^2)$ and $F_2^\gamma(x, Q^2)$:

$$\frac{d^5\sigma}{dz_1\, dz_2\, d\cos\theta_1\, d\cos\theta_2\, d\phi} = \frac{d^5 L_{\gamma\gamma}^{TT}}{dz_1\, dz_2\, d\cos\theta_1\, d\cos\theta_2\, d\phi} \cdot \frac{8\pi^2\alpha}{Q^2(1+(1-y)^2)} \cdot \{(1-y)F_2^\gamma(x, Q^2) + xy^2 F_1^\gamma(x, Q^2)\} \tag{2}$$

where z_1, z_2 are the normalized photon energies $z_i = E_{\gamma i}/E_b$, θ_1, θ_2 the lepton scattering angles and ϕ the azimuthal angle between the $e^+e^{+\prime}-$ and the $e^-e^{-\prime}$ scattering planes. $L_{\gamma\gamma}^{TT}$ represents the flux of two transversely polarized photons. For this analysis $L_{\gamma\gamma}^{TT}$ was taken from [4]. The variables Q^2, x and y are given by

$$\begin{aligned} Q^2 &= 4E' E_b \sin^2(\theta_1/2) = -q^2 \\ y &= 1 - E'/E_b \cos^2(\theta_1/2) \\ x &= \frac{Q^2}{Q^2 + W_{\gamma\gamma}^2} \end{aligned} \tag{3}$$

with E' being the energy of the tagged lepton and $W_{\gamma\gamma}$ the invariant mass of the colliding photons.

Because of the cuts imposed on E' and θ_1 in this experiment, y is small with an average value of $\langle y \rangle = 0.2$ and $\langle xy^2 \rangle = 0.03$. The contribution of F_1^γ in (2) is thus negligible.

Usually F_2^γ is considered as a sum of a pointlike and a so called 'hadronic' part. Walsh and Zerwas [5] suggested that at large Q^2 the photon structure function is dominated by the pointlike contribution from the direct $\gamma\gamma \to q\bar{q}$ coupling which can be calcu-

[1] Now at Siemens, München, FRG
[2] Now at Philipps, Aachen, FRG
[3] Now at Fraunhofer Institut, Duisburg, FRG
[4] On leave from Weizmann Institute, Rehovot, Israel
[5] On leave from Institute of Nuclear Physics, Cracow, Poland
[6] Now at IPP Canada, Carleton University, Ottawa, Canada
[7] Now at Warsaw University, Warsaw, Poland
[8] On leave from Warsaw University, Warsaw, Poland
[9] Now at GKSS, Geesthacht, FRG
[10] Now at CERN, Geneva, Switzerland
[11] Now at University of Malaya, Kuala Lumpur, Malaysia
[12] Now at British Telecomm, Great Britain
[13] On leave from Universidad Autonoma de Madrid, Madrid, Spain
[14] Now at Lawrence Berkeley Laboratory, Berkeley, CA, USA
[15] Now at University of Illinois, Urbana-Champaign, USA
[16] Now at Yale University, New Haven, CT, USA
[17] Now at California Institute of Technology, Pasadena, CA, USA
[18] Supported by the Bundesministerium für Forschung und Technologie
[19] Supported by the UK Science and Engineering Research Council
[20] Supported by CAICYT
[21] Supported by the Minerva Gesellschaft für Forschung mbH
[22] Supported by the US Department of Energy, contract DE-AC02-76ER00881 and by the U.S. National Science Foundation Grant Number INT-8313994 for travel

lated in the Quark Parton Model, QPM, [5] or under certain theoretical assumptions in perturbative Quantum Chromodynamics, QCD [6].

In the quark parton model F_2^γ is given (for u, d, s quarks) [5, 7] by:

$$F_2^{\gamma\,\mathrm{QPM}}(x, Q^2) = 3\sum e_q^4 \cdot \frac{\alpha}{\pi}\left\{x(x^2+(1-x)^2)\ln\frac{W_{\gamma\gamma}^2}{m_q^2} + 8x^2(1-x) - x\right\} \tag{4}$$

where e_q, m_q are the quark charges and masses respectively.

The contribution of the c quark to F_2^γ, taking proper account of the large c quark mass, m_c, is given in [7]:

$$F_2^{\gamma c\bar{c}} = x\cdot\frac{3\alpha}{\pi}e_q^4\left\{\Delta\left(8x(1-x)-1-4\frac{m_c^2}{Q^2}\cdot x(1-x)\right) + \left(x^2+(1-x)^2+4\frac{m_c^2}{Q^2}x(1-3x)-8\frac{m_c^4}{Q^4}x^2\right)\ln\frac{1+\Delta}{1-\Delta}\right\} \tag{5}$$

with $\Delta^2 = 1-\dfrac{4m_c^2 x}{(1-x)Q^2}$.

In leading order QCD (LOQCD) F_2^γ has been calculated for light quarks $q(u, d, s)$ in [6]:

$$F_2^{\gamma\,\mathrm{LO}}(x, Q^2) = \frac{3\alpha}{\pi}\sum e_q^4 f^{\mathrm{LO}}(x)\ln\frac{Q^2}{\Lambda_{\mathrm{LO}}^2}. \tag{6}$$

A higher order calculation (HOQCD) in [8] (using the $\overline{\mathrm{MS}}$-scheme) gives:

$$F_2^{\gamma\,\mathrm{HO}}(x, Q^2) = \frac{3\alpha}{\pi}\sum e_q^4\left\{f(x)\ln\frac{Q^2}{\Lambda_{\overline{\mathrm{MS}}}^2} + g(x)\ln\left(\ln\frac{Q^2}{\Lambda_{\overline{\mathrm{MS}}}^2}\right) + h(x)\right\}. \tag{7}$$

In (6) and (7) $f^{\mathrm{LO}}(x)$, $f(x)$, $g(x)$, $h(x)$ are known functions and e_q are the fractional charges of the quarks*.

Equations (6), (7) show that the QCD parameter Λ_{LO} or $\Lambda_{\overline{\mathrm{MS}}}$, can be determined directly from the magnitude of $F_2^\gamma(x, Q^2)$. However, this method of determining Λ poses problems which are still debated [10–12]. The arbitrary separation of F_2^γ into a hadronic and a pointlike part leads in next-to-leading order to negative values of the perturbatively calculable part of F_2^γ at small x with a singularity at $x=0$. In [11] a procedure is suggested to regularize F_2^γ at small x and it is shown that the perturbative calculation is reliable for $x>0.2$.

* At the high Q^2 values of this experiment a gauge invariant quark model with integer quark charges yields nearly the same magnitude of F_2^γ as given by (6) and (7) [9]

In the present paper the hadronic part of F_2^γ, F_2^{HAD}, was estimated assuming vector meson dominance [10], where F_2^{HAD} was inferred from measurements of the pion structure function, leading, for the light quark contributions, to:

$$F_2^{\gamma\,\mathrm{HAD}} = 0.2\cdot\alpha\cdot(1-x). \tag{8}$$

The contribution from charmed quarks was obtained by assuming J/ψ dominance [13]:

$$F_2^{\gamma\,J/\psi}(x) = \left(\frac{e_q}{f_\psi}\right)^2\cdot\frac{2}{3}\sqrt{x}(1-x) \tag{9}$$

where f_ψ^2 is given by $f_\psi^2 = \dfrac{4\pi}{3}\alpha^2\dfrac{m_{J/\psi}}{\Gamma(J/\psi\to e^+e^-)}$.

3. Experimental Procedure

3.1. Detector Components

The general description of the TASSO detector has been given in [14]. The charged tracks of the hadronic system of reaction (1) were measured in the central drift and proportional chambers, which cover a solid angle of 87% of 4π. Photons and electrons were detected in the liquid argon endcap shower counters (LAEC) [15], the liquid argon barrel counters (LABC) [16], and the hadron arm lead-scintillator sandwich shower counters (HASH) [17], covering in total a solid angle of 65% of 4π.

The scattered electrons which tagged the high q^2 photons were measured in the LAEC, which cover a polar angular range of 13.2–28.7°, and 151.3–166.8° and all azimuthal angles. The calorimeter consists of small front towers (depth 5.9 radiation length, X_0, $\Delta\Omega = 8$ msr) followed by back towers (depth: $7.6X_0$) each covering 4 front towers. In order to improve the position measurement of showers, the calorimeter contains two planes of readout strips which are oriented along lines $R=$const (R-strips) and $\phi=$const (ϕ-strips) at two different depths $0.7X_0$ and $2.9X_0$. A detailed description of the experimental setup and the electronics is given in [15]. Electrons (and photons) were found by a pattern recognition program which scans the information of the calorimeter for energy clusters. A cluster was defined as a group of adjacent front towers each with an energy deposit larger than 20 MeV. The cluster search started from local energy maxima in the front towers. The energy of all adjacent front towers was added as long as this energy decreased. Detecting an energy increase led to a new cluster. Any energy deposited in the back towers was added to the energy measured in the associated front towers.

The r.m.s. energy resolution σ_E/E can be parame-

trized by $0.10/\sqrt{E}+0.03$ as checked with Bhabha scattering events at beam energies between 11 GeV and 17.5 GeV. The precise position of the cluster was determined from small towers and R- and ϕ-strips using the center of gravity method. The measured angular resolutions obtained from high energy Bhabha events were $\sigma_\theta=2$ mrad and $\sigma_\phi=6.5$ mrad. The performance of the calorimeter was constantly monitored using Bhabha scattering.

3.2. Event Selection

The trigger demanded at least one cluster in the LAEC with an energy greater than 1.5 GeV and at least one charged track in the inner detector with $|\cos\theta|<0.82$ and a transverse momentum $p_t>0.3$ GeV/c with respect to the beam axis.

For the event reconstruction charged tracks were accepted if they had $p_t>0.1$ GeV/c and $|\cos\theta|<0.87$. These tracks had to originate within 20 cm of the interaction point along the beam axis, and within 5 cm in a plane perpendicular to the beam. Photons were required to have energies larger than 0.15 GeV in the LAEC and LABC, and larger than 0.25 GeV in the HASH.

The following event selection criteria were applied:

a) A cluster in the LAEC polar angle range with an energy greater than 9 GeV was demanded. It was not explicitly required that the cluster originated from a charged track.

b) To keep the four momentum squared of the target photon, p^2, as small as possible we restricted the second $e^\pm$ to small polar angles by requiring that there were no additional clusters in the LAEC, LABC and HASH with an energy $E>5$ GeV (anti-tag condition).

c) Three or more charged tracks were demanded, one of which with $p_t>0.3$ GeV/c and $|\cos\theta|<0.8$. At least two of the charged tracks were required to be separated by more than 30°. These cuts discriminated against the QED reactions $e^+e^-\to l^+l^-+\gamma$ and $e^+e^-\to e^+e^-+l^+l^-$ with l^+l^- being the leptons e, μ and τ.

d) To suppress 1γ annihilation events, the total energy of the hadronic final state E_{had} was required to be less than the beam energy. The invariant mass W_{vis} of the detected hadronic system was required to be greater than 1 GeV. Both, W_{vis} and E_{had} were calculated from the measured momenta of the charged tracks (assuming pion masses) and of the photons.

e) A further discrimination against 1γ annihilation events was achieved by the following requirements:

– transverse momentum balance (with respect to the beam)

$$|\mathbf{p}_t^{\text{tag}}-\mathbf{p}_t^{\text{had}}|<3 \text{ GeV/c},$$

– missing longitudinal momentum (associated with the undetected electron)

$$|p_{//}^{\text{tag}}-p_{//}^{\text{had}}|>7 \text{ GeV/c},$$

where $\mathbf{p}_t^{\text{tag}}$ and $p_{//}^{\text{tag}}$ are the transverse and longitudinal momentum of the measured electron, and $\mathbf{p}_t^{\text{had}}$, $p_{//}^{\text{had}}$ the transverse and longitudinal components of the vector sum of the charged hadron and photon momenta, respectively.

f) The contamination from beam gas scattering was reduced by demanding $|Z_{\text{vert}}-Z_0|<6$ cm where Z_{vert} is the reconstructed event vertex and Z_0 the nominal interaction point.

After these cuts 344 events remained.

3.3. Background

Using Monte Carlo programs, the contributions from the following background processes were calculated:

a) Inelastic Compton scattering [10]:

5 ± 0.5 events (1.5%)

b) $e^+e^-\to e^+e^-+\tau^+\tau^-$:

30 ± 3.5 events (9%).

c) $e^+e^-\to\tau^+\tau^-$, where one of the τ leptons decayed into an electron which fulfilled the tag criteria, and the other τ decayed to hadrons:

3 ± 1 events (1%).

d) Hadronic events from 1γ annihilation, where an initial state bremsstrahlung γ or a γ from π° decay fulfills the tag criteria:

44 ± 3.5 events (13%).

The amount of the latter background was considerable, because it was not required that the tag cluster originated from a charged track.

The residual background originating from beam gas interactions was determined from the data by using the side bands of the event vertex distribution along the beam. It was found to be negligible (<1%).

The background contributions sum to 82 ± 5 (stat) ±8 (syst) events ($24\%\pm1.5\%\pm2.5\%$), where the estimated systematic error originates mainly from the uncertainty in the simulation model for the 1γ annihilation processes.

After subtraction of these background contributions, a sample of $262\pm19\pm8$ events attributed to process (1) remained.

4. Analysis

4.1. Experimental Distributions

Figures 1-3 show the Q^2_{vis}, W_{vis} and x_{vis} ($x_{vis} = Q^2_{vis}/(Q^2_{vis} + W^2_{vis})$) distributions of the data together with the background events. The mean Q^2_{vis} value for the background subtracted data is $\langle Q^2_{vis} \rangle = 23$ (GeV/c)^2. As determined by Monte Carlo calculations, the ratio of the measured Q^2_{vis} to the true Q^2 has an average value of 1 with an 8% spread. The invariant mass of the colliding photons, $W_{\gamma\gamma}$, is calculated from the momenta and energies of the particles of the hadronic final state. Due to acceptance losses the calculated visible invariant mass, W_{vis}, is systematically shifted to smaller values (on average 36%) with respect to the true mass $W_{\gamma\gamma}$. As a consequence, the calculated value x_{vis} is shifted to larger values $x_{vis} > x$.

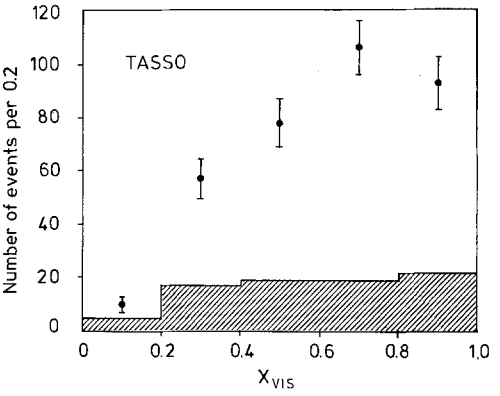

Fig. 3. Observed x distribution $x_{vis} = Q^2_{vis}/(Q^2_{vis} + W^2_{vis})$ before background subtraction. The shaded histogram represents the background

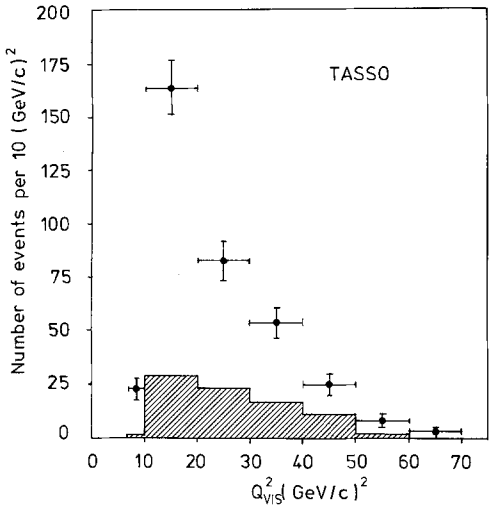

Fig. 1. Observed Q^2 distribution (Q^2_{vis}) before background subtraction. The shaded histogram represents the background

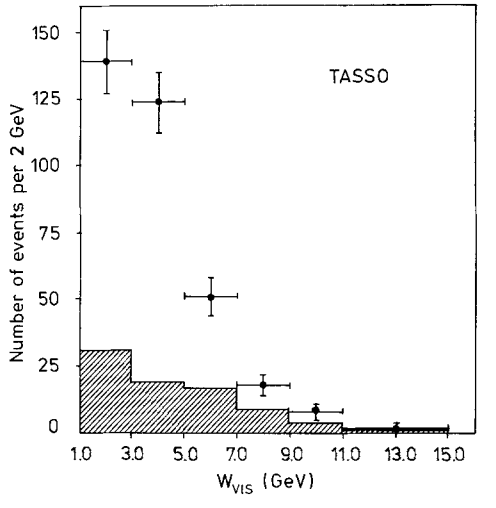

Fig. 2. Observed distribution of the invariant mass (W_{vis}) of the hadronic system before background subtraction. The shaded histogram represents the background

Comparing the data with theoretical models requires either an unfolding procedure for the variable x, or the comparison in the visible quantities. We used both ways in our analyses. We first compared the observed x_{vis} distribution to the theoretical predictions. These predictions were obtained by means of a Monte Carlo program [18] which generated hadronic two-photon events for a given F_2^γ. In the second approach, F_2^γ was determined at an average value of Q^2 by unfolding the measured x_{vis} distribution. Then $F_2^\gamma(x)$ was compared to the various theoretical predictions.

4.2. Monte Carlo Simulation

The Monte Carlo simulation was done in the following way. First events of the type $e^+e^- \to e^+e^- + q\bar{q}$ were generated following (2) and using theoretical predictions for F_2^γ.

The following models were used for the structure function F_2^γ:

a) QPM with or without a hadronic part (8); (4) for light quarks (u, d, s), and the c quark contribution as described in Chap. 1. Equation (5) was modified between the maximum of F_2^γ and the $c\bar{c}$ threshold to account for QCD corrections [13].

b) LOQCD as in (6) following a calculation of [10] with a hadronic part (8) and the same c quark contribution as in model a).

c) HOQCD as in (7) following a calculation of [19]* plus a hadronic part (8). The c quark was treated as in model a).

* For negative values of the photon structure function, F_2^γ was set to zero

The QPM and QCD calculations hold only under the assumption that the four momentum squared of the target photon, p^2, fulfills the condition $|p^2| \ll m_q^2$ or $|p^2| \ll \Lambda^2$, where m_q is the quark mass and Λ is the QCD scale parameter, respectively. For our antitag condition, no additional electron at a polar angle $\theta_e > 210$ mrad and an energy larger than 5 GeV (see 3.2b), $|p^2| \neq 0$ can occur. For $|p^2| \gg \Lambda^2$ the scale of the q^2 dependence of F_2^γ is given by p^2 instead of Λ^2.

In this case F_2^γ is exactly calculable in QCD according to [20]. Since the value of p^2 cannot be measured, its effect was taken into account in the Monte Carlo simulation. In the QCD models we replaced Λ^2 by $\Lambda^2 + |p^2|$ and in the QPM m_q^2 by $m_q^2 + |p^2|$. For $F_2^{\gamma \mathrm{HAD}}$ the right hand side of (8) was multiplied by a propagator term of the form $m_\rho^2/(m_\rho^2 + |p^2|)$. The simulation showed that for 75% of the events $|p^2| < 0.01$ (GeV/c)^2.

For the pointlike part a parametrization of the angular distribution of the $q\bar{q}$ pairs with respect to the $\gamma\gamma$ direction in the $\gamma\gamma$ CM system was determined by using a computer program [21] taking into account the squared four-momentum transfer values, q^2, p^2.

For the hadronic part, the $q\bar{q}$ pair was oriented along the $\gamma\gamma$ directions. Quark flavors were generated with quark masses $m_u = m_d = m_s = 300$ MeV/c^2, $m_c = 1{,}550$ MeV/c^2.

Radiative corrections were taken into account by a correction factor of 1.04 estimated from [22].

The hadronization of the $q\bar{q}$ system was done according to the following model:

a) For $W_{\gamma\gamma} < 4$ GeV a multipion phase space model was used with limited transverse momentum with respect to the quark direction [23]. The multiplicity of the pions was chosen to be Poisson distributed with a mean of $\langle n \rangle = 1.7 \cdot (2.0 + 1.4 \ln W)$, motivated by low energy measurements in $e^+ e^-$ annihilation. The ratio of charged to neutral pions was taken to be 1:1.22. The distribution of transverse momenta p_t relative to the $\gamma\gamma$ axis, dN/dp_t^2, was taken to be proportional to $e^{-\alpha p_t^2}$ with a mean value $\langle p_t \rangle$ of 420 MeV/c.

b) For $W_{\gamma\gamma} > 4$ GeV we used the Field Feynman (FF) fragmentation scheme [24] with the following fragmentation functions and parameters: for light (u, d, s) quarks we used the standard FF fragmentation function [24] with $a_F = 0.77$ and for the c quark we used the fragmentation [25] with $\varepsilon_c = 0.18$ [26]. The values of the other parameters were taken as [27] $\sigma_q = 320$ MeV/c, $P/(P+V) = 0.5$, $u:d:s = 2:2:1$ and the probability to create a diquark in the cascade was taken as 0.075.

The generated hadrons were passed through the detector simulation taking into account all efficiencies and resolutions. The Monte Carlo events had to pass the same cuts as the real data. The model describes well those features of the data which are sensitive to the fragmentation scheme. This is demonstrated in Figs. 4a–c, where the distributions of the charged and neutral multiplicity and the transverse momentum squared (with respect to the beam axis) are shown.

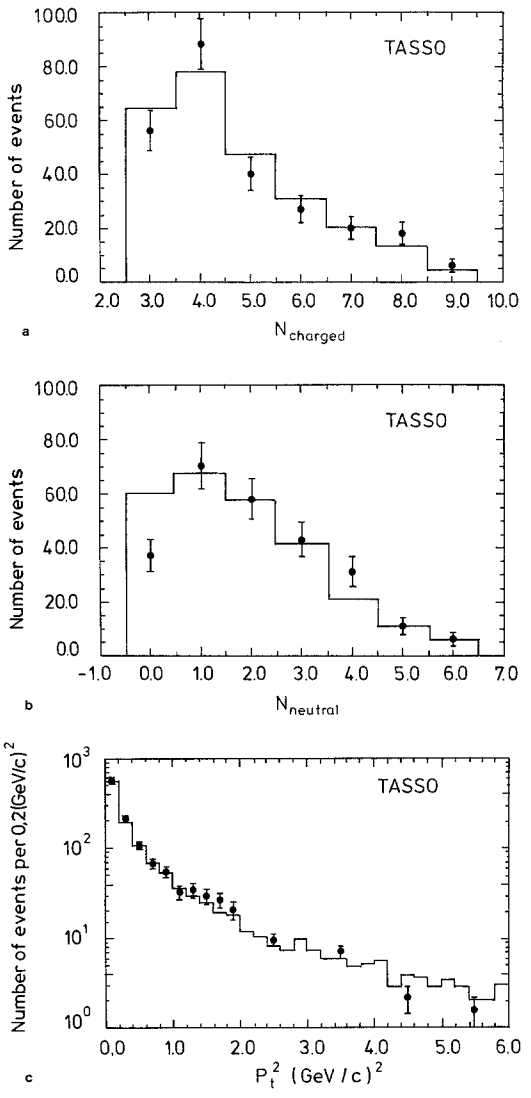

Fig. 4a–c. Comparison of the data with Monte Carlo calculations for distributions sensitive to fragmentation. The histograms represent the Monte Carlo predictions for the model LOQCD (u, d, s) with $\Lambda_{\mathrm{LO}} = 150$ MeV including the hadronic part and the c quark contribution. **a** Multiplicity of charged particles with $p_t > 100$ MeV/c, p_t being the transverse momentum with respect to the beam axis. **b** Multiplicity of photons with energies greater than 150(250) MeV in the LAEC, LABC (HASH) detectors. **c** p_t^2 distribution of charged particles, p_t^2 being the transverse momentum squared with respect to the beam axis

4.3. *Comparison of the x_{vis} Distribution with Models*

In Figs. 5a–c, we show the background corrected x_{vis} distribution ($x_{vis}=Q^2_{vis}/(Q^2_{vis}+W^2_{vis})$). The error bars on the data points are statistical only.

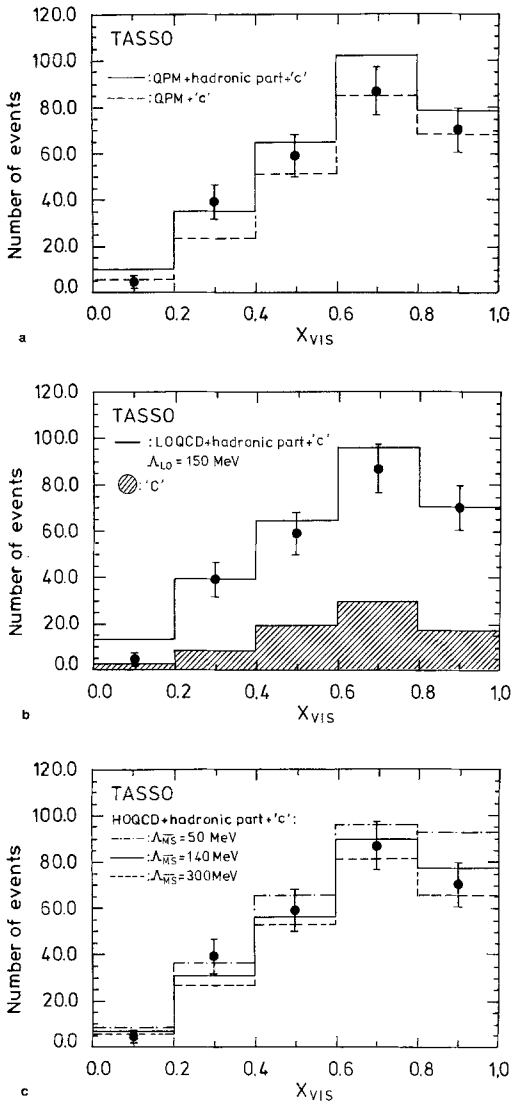

Fig. 5a–c. Comparison of the data with model predictions in the x_{vis} distribution. **a** The dashed histogram represents the Monte Carlo prediction for QPM (u, d, s) including the c quark contribution. The solid histogram gives the prediction of the Monte Carlo for QPM (u, d, s) including the c quark contribution and the hadronic part. **b** The solid histogram represents the Monte Carlo prediction for LOQCD (u, d, s) including the c quark contribution and the hadronic part with $\Lambda_{LO}=150$ MeV. The shaded histogram represents the c quark contribution calculated following (5) and (9). **c** The histograms represent the Monte Carlo prediction for HOQCD (u, d, s) including the c quark contribution and the hadronic part for different $\Lambda_{\overline{MS}}$ values. The dashed histogram is for $\Lambda_{\overline{MS}}=300$ MeV, the dashed-dotted histogram for $\Lambda_{\overline{MS}}=50$ MeV and the solid histogram for the best fit value, $\Lambda_{\overline{MS}}=140$ MeV

Figure 5a shows the comparison with the QPM (dashed line). Including the hadronic part (solid line) the data are well described. Figure 5b shows the comparison with LOQCD using $\Lambda_{LO}=150$ MeV. The dashed area shows the contribution of the c quark, calculated following (5) and (9); it amounts to 28%. A comparison with HOQCD is shown in Fig. 5c. The dashed histogram represents the HOQCD calculation for $\Lambda_{\overline{MS}}=300$ MeV whereas the dashed-dotted histogram is for $\Lambda_{\overline{MS}}=50$ MeV, indicating the sensitivity to $\Lambda_{\overline{MS}}$. A least squares fit of $\Lambda_{\overline{MS}}$ using the higher order calculation, yields:

$$\Lambda_{\overline{MS}}=140^{+90}_{-35}\ \text{MeV}.$$

The errors are purely statistical. The corresponding distribution is shown as the solid histogram of Fig. 5c.

The comparison of the x distribution with the three models in Figs. 5a–c shows that it is not possible to distinguish between these models.

Systematic uncertainties of the x_{vis} distribution come from the following sources: the luminosity measurement (4%), the radiative corrections (2%), and the background contribution (3%) adding up to ±5.5%. Errors coming from uncertainties in the determination of the fragmentation parameters and the detector acceptance and resolutions were estimated by Monte Carlo simulation to be ±10%. Other contributions to the systematic error come from the treatment of the hadronic part in F_2^γ, the c quark contribution and the nonzero value of p^2. The uncertainties from these three sources were estimated to be ±8%, ±7% and ±10%, respectively.

Altogether this gives a total systematic uncertainty of ±19%. Adding this error in quadrature (point to point in the x_{vis}-distribution) to the statistical error and performing again a fit of $\Lambda_{\overline{MS}}$, the following value was obtained:

$$\Lambda_{\overline{MS}}=140^{+190}_{-\ 65}\ \text{MeV}.$$

The main assumptions which were made to derive the $\Lambda_{\overline{MS}}$ value are as follows:

1. The pointlike part calculated in HOQCD and the hadronic part estimated by [10] can be added incoherently.

2. The four momentum squared of the target photon can be treated as described above.

3. The c quark contribution is taken as proposed in [13].

4.4. Determination of the Structure Function F_2^γ

In order to allow a direct comparison with theoretical predictions, we determined F_2^γ by unfolding the x_{vis} into the x distribution following a method explained in [28]. The mapping of x to x_{vis} was done by a Monte Carlo simulation and then inverted in such a way as to avoid the enhancement of fluctuations usually occuring in the calculation of matrix inversions.

The unfolding was done in the x variable alone. In order to check the influence of a Q^2 dependence on the unfolding procedure a factorization ansatz of F_2^γ in x and Q^2, $F_2^\gamma(x, Q^2) = F_2^\gamma(x)\{1 + a \ln Q^2/\langle Q^2\rangle\}$ was tried. We found that within the statistical errors the unfolding in x alone was sufficient.

The reliability of the unfolding procedure was checked as follows: First Monte Carlo events were generated which used either the QPM (4) or the hadronic part (8) as a model for F_2^γ. The resulting x_{vis} distributions in both cases were then unfolded using the normal procedure and the unfolded values for F_2^γ were compared to the input models. Figures 6a, b show that for the two very different shapes the unfolded distributions agree well with the input distributions.

In order to obtain an unfolded structure function for target photons with $p^2 = 0$ (rather than presenting an integral of F_2^γ over the accepted p^2 distribution), the effect of the nonzero values of p^2 was taken into account in the unfolding procedure. For the input structure function the p^2 dependence was parametrized as described in 4.2. The Λ value had to be fixed for the unfolding calculations: we chose $\Lambda_{\overline{MS}} = 140$ MeV. The effect of the nonzero p^2 is substantial. Neglecting it, i.e. $p^2 = 0$, would decrease the unfolded structure function by $\sim 20\%$.

Figure 7 shows the unfolded structure function

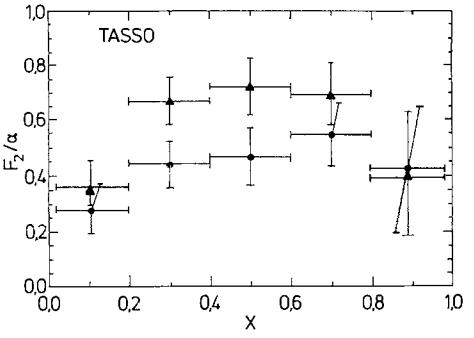

Fig. 7. The unfolded structure function $F_2^\gamma(x)$ at $Q^2 = 23$ (GeV/c)^2 (triangles). The circles represent F_2^γ for the light quarks, i.e. the theoretical c quark contribution is subtracted

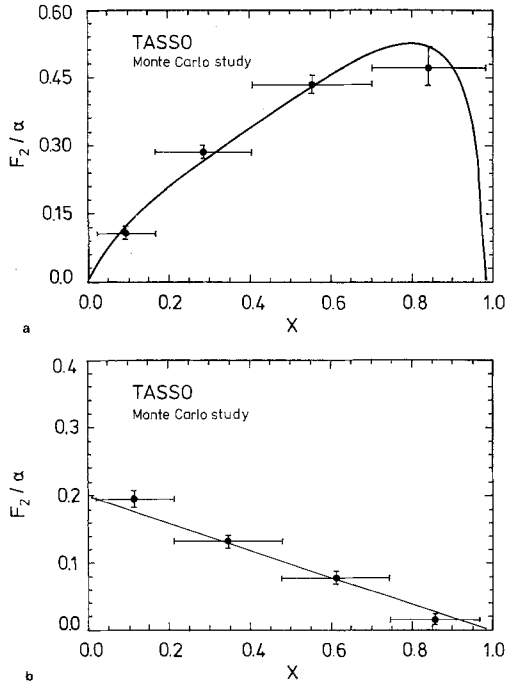

Fig. 6a, b. Study of the reliability of the unfolding procedure: The input functions are the solid curves. The points with the (statistical) errors represent the results of the unfolding after the detector simulation. **a** Input function for F_2^γ: QPM (4). **b** Input function for F_2^γ: hadronic part (8)

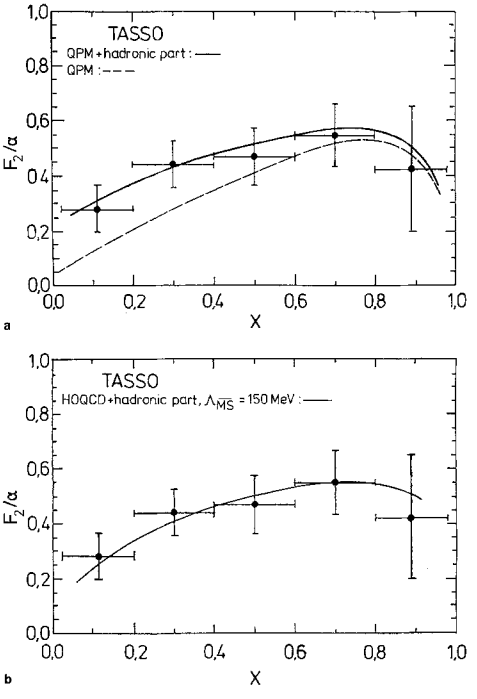

Fig. 8a, b. Comparison of the unfolded structure function $F_2^\gamma(x)$ (theoretical c quark contribution subtracted) with models: **a** The dashed curve represents the QPM prediction for u, d, s quarks, the solid curve the predictions for QPM (u, d, s) including the hadronic part. **b** The curve represents the HOQCD prediction for u, d, s quarks for $\Lambda_{\overline{MS}} = 150$ MeV including the hadronic part

$F_2^\gamma(x, Q^2 = 23\ (\mathrm{GeV/c})^2)$ (triangles). The full dots represent F_2^γ for the light quarks only, where the c quark contribution has been subtracted in the unfolding procedure using formulae (5) and (9).

The computed charm contribution has also been subtracted in the following figures. In Fig. 8a F_2^γ is compared with the theoretical predictions of the QPM (solid line) and the QPM + hadronic part (dashed line). Figure 8b shows the comparison between F_2^γ and the prediction of HOQCD + hadronic part. Here the parametrization of [19] with $\Lambda_{\overline{\mathrm{MS}}} = 150$ MeV and (8) were used, respectively. This value has been determined by a fit to the unfolded distribution and compares well with the value extracted from the x_{vis} distribution. The QPM and HOQCD, both with the hadronic part included, describe the data almost equally well.

5. Conclusion

A measurement of the photon structure function F_2^γ has been carried out using events of the process $e^+e^- \to e^+e^-$ + hadrons under the single tag condition. The Q^2 range was $7 < Q^2 < 70$ (GeV/c)^2 with a mean value of 23 (GeV/c)^2. A total of 262 events were attributed to this process. The data were analysed in two ways. In the first one different theoretical models were compared with the data in the x_{vis} distribution. The second method used the unfolded structure function F_2^γ for a comparison with the theoretical predictions. Both methods gave consistent results.

The data agree within the errors with the sum of the QPM and a hadronic part using quark masses of 300 MeV/c^2 for the light quarks. They are also in agreement with leading order QCD or higher order QCD calculations, both with the hadronic part included. Under the assumptions listed in Chap. 4 a value for the higher order QCD scale parameter $\Lambda_{\overline{\mathrm{MS}}}$ was obtained by a fit to the x_{vis} distribution yielding

$$\Lambda_{\overline{\mathrm{MS}}} = 140\ ^{+90}_{-35}\ \mathrm{MeV},$$

where the errors are purely statistical. Including the systematic errors we got

$$\Lambda_{\overline{\mathrm{MS}}} = 140\ ^{+190}_{-\ 65}\ \mathrm{MeV}.$$

This result agrees within errors with previous determinations of the photon structure functions [1, 2].

Acknowledgements. We thank Messrs. M. Buchholz, M. Dohmen, V. Kadansky, G. Peise, G. Plümecke, J. Rimkus, R. Siedling, H. Vennemann and G. Wertz from the I. Physikalisches Institut der RWTH Aachen and Messrs. J. Bengtson, R. Hensler and D. Hubert from DESY for the superb work they have done during construction and testing of the stacks and the electronics of the liquid argon endcap calorimeters.

We gratefully acknowledge the effort of the PETRA machine group, the DESY computer centre and the support of the DESY directorate. We are grateful to P.M. Zerwas and V. Blobel for many helpful discussions. Those of us from outside DESY wish to thank the DESY directorate for the hospitality extended to us while being at DESY.

References

1. PLUTO Collab. Ch. Berger et al.: Phys. Lett. **107 B**, 168 (1981); PLUTO Collab. Ch. Berger et al.: Phys. Lett. **142 B**, 111 (1984)
2. JADE Collab. W. Bartel et al.: Phys. Lett. **121 B**, 203 (1983); JADE Collab. W. Bartel et al.: Z. Phys. C – Particles and Fields **24**, 231 (1984)
3. CELLO Collab. H.J. Behrend et al.: Phys. Lett. **126 B**, 391 (1983)
4. J.H. Field: Nucl. Phys. **B 168**, 477 (1980); Erratum, Nucl. Phys. **B 176**, 545 (1980)
5. T.F. Walsh, P.M. Zerwas: Phys. Lett. **44 B**, 195 (1973)
6. E. Witten: Nucl. Phys. **B 120**, 189 (1977)
7. V.M. Budnev, I.F. Ginzburg, G.V. Meledin, V.G. Serbo: Phys. Rep. **C 15**, 4 (1975)
8. W.A. Bardeen, A.J. Buras: Phys. Rev. **D 20**, 166 (1979); D.W. Duke, J.F. Owens: Phys. Rev. **D 22**, 2280 (1980)
9. R.M. Godbole et al.: Phys. Lett. **142 B**, 91 (1984)
10. C. Peterson, T.F. Walsh, P.M. Zerwas: Nucl. Phys. **B 174**, 424 (1980); C. Peterson, T.F. Walsh, P.M. Zerwas: Nucl. Phys. B **229**, 301 (1983)
11. I. Antoniadis, G. Grunberg: Nucl. Phys. **B 213**, 445 (1983); I. Antoniadis, L. Marleau: SLAC-Pub-3691 (1985)
12. M. Glück, E. Reya: Phys. Rev. **D 28**, 2749 (1983); C. Peterson, T.F. Walsh, P.M. Zerwas: Nucl. Phys. **B 229**, 301 (1983); M. Glück, K. Grassie, E. Reya: Phys. Rev. **D 30**, 1447 (1984); G. Rossi: Phys. Lett. **130 B**, 105 (1983); G. Rossi: Univ. of California (Santa Barbara) Preprint UCSB-TH1 (1983); W.A. Bardeen, Talk given at the VI $\gamma\gamma$-Workshop Lake Tahoe 1984, and Fermilab-Conference 84/133-I (1984)
13. I. Schmitt: Talk given at the V. Int. Workshop on $\gamma\gamma$-Collisions, Aachen 1983, summarized by D.M. Scott, Proc. of the V. Int. Workshop on Photon Photon Collisions, Aachen 1983, ed. Ch. Berger, Springer Verlag (1983); P.M. Zerwas, private communication
14. TASSO Collab. R. Brandelik et al.: Phys. Lett. **83 B**, 261 (1979)
15. V. Kadansky et al.: Phys. Scr. **23**, 680 (1981)
16. TASSO Collab. R. Brandelik et al.: Phys. Lett. **108 B**, 71 (1982)
17. TASSO Collab. R. Brandelik et al.: Phys. Lett. **92 B**, 199 (1980)
18. F.J. Kirschfink: Thesis, Aachen, PITHA 84/40 (1984)
19. D.W. Duke, private communication, based on [8]
20. T. Uematsu, T.F. Walsh: Phys. Lett. **101 B**, 263 (1981); T. Uematsu, T.F. Walsh: Nucl. Phys. **B 199**, 93 (1982)
21. J.A.M. Vermaseren: Talk given at the Int. Colloquium on $\gamma\gamma$-Collisions, Amiens, Lecture Notes in Physics No. 134 (1980)
22. W.L. Van Neerven, J.A.M. Vermaseren: Nucl. Phys. **B 238**, 73 (1984)
23. O. Pene, A. Krzywicki: Nucl. Phys. **B 12**, 415 (1969)
24. R.D. Field, R.P. Feynman: Nucl. Phys. **B 136**, 1 (1978)
25. C. Peterson et al.: Phys. Rev. **D 27**, 105 (1983)
26. TASSO Collab. M. Althoff et al.: Phys. Lett. **126 B**, 493 (1983)
27. TASSO Collab. R. Brandelik et al.: Phys. Lett. **94 B**, 437 (1980)
28. V. Blobel: DESY 84-118 (1984)